Received: 31 May 2022 | Revised: 15 September 2022 | Accepted: 21 October 2022

DOI: 10.4218/etrij.2022-0207

SPECIAL ISSUE

ETRI Journal WILEY

Frequency divided group beamforming with sparse space-frequency code for above 6 GHz URLLC systems

Chanho Yoon | **Woncheol Cho** | **Kapseok Chang** | **Young-Jo Ko**

Telecommunications and Media Research Laboratory, Electronics Telecommunications Research Institute, Daejeon, Republic of Korea

Correspondence
Chanho Yoon, Telecommunications and Media Research Laboratory, Electronics Telecommunications Research Institute, Daejeon, Republic of Korea.
Email: chyoon@etri.re.kr

Funding information
This research was supported by the Institute of Information Communications Technology Planning Evaluation, grant/award number: 2018-0-00218

Abstract

In this study, we propose a limited feedback-based frequency divided group beamforming with sparse space-frequency transmit diversity coded orthogonal frequency division multiplexing (OFDM) system for ultrareliable low latency communication (URLLC) scenario. The proposed scheme has several advantages over the traditional hybrid beamforming approach, including not requiring downlink channel state information for baseband precoding, supporting distributed multipoint transmission structures for diversity, and reducing beam sweeping latency with little uplink overhead. These are all positive aspects of physical layer characteristics intended for URLLC. It is suggested in the system to manage the multipoint transmission structure realized by distributed panels using a power allocation method based on cooperative game theory. Link-level simulations demonstrate that the proposed scheme offers reliability by achieving both higher diversity order and array gain in a non-line-of-sight channel of selectivity and limited spatial scattering.

KEYWORDS
above 6 GHz, hybrid beamforming, power allocation, URLLC, 6G

1 | INTRODUCTION

It is anticipated that the fifth generation (5G) New Radio (NR) wireless system will support a variety of specialized services in real-world scenarios of vertical domains like factory automation, automotive controls, e-health care, smart metering, and tactile internet. In such machine-type communication (MTC), the aspect will play a significant role in the future beyond 5G networks [1, 2]. The ultrareliable low latency communications (URLLC) service class introduced in the 5G NR can be used to implement mission-critical MTC among the other MTC services. URLLC service class caters to mission-critical applications with strict quality of service requirements. For instance, the codeword block error rate for a URLLC application intended for factory automation in the post-5G era suggests that there are strict requirements block error rate (BLER) of 10^{-9} and submillisecond end-to-end latency [3–8].

Wireless communications that are ultrareliable and low latency demand design objectives that call for significant physical transmission technique design to combat erratic wireless channel behavior. There are significant obstacles that physical layer design must get around to make it possible for URLLC network services to be deployed in the millimeter wave (mmWave) bands. Examples of this include dealing with cell-to-cell interference and high signal propagation loss in free space in channel environments. The former could be partially compensated by applying beamforming with tightly

packed antenna arrays having high levels of antenna correlation, and the latter could be mitigated or/and avoided by deploying multipoint transmission method or adaptive neighboring cell scheduling combined with beamforming to improve the SINR.

Recent research and practice have focused on a technique known as hybrid beamforming, which uses large antenna arrays at both the transmitter and receiver along with baseband precoding and combining techniques [9–16]. The suggested method deviates from earlier works in that a hybrid beamforming technique is used. The assessed model of channel structure is strictly limited to the baseband model that analog beamforming before digital beamforming is assumed, whereas the previous works model antenna element level channel structure and precoding. Even though the hybrid beamformer's digital precoder dimension is much smaller than its analog domain counterpart, accurate knowledge of the downlink channel coefficients at the radio frequency (RF) chain matrix level is necessary for the transmitter to operate at its best. All possible combinations of the analog domain of massive antenna elements, which are typically adjusted by a phase shifter network and digital precoding result in a nonconvex optimization problem that must be solved.

For the URLLC environment, searching optimal solution for a combined precoding matrix and analog phase shifter accounting for extended beam sweeping duration may not be delay efficient. For large antenna arrays, heavy overhead is needed for this two-stage feedback for both the RF beamforming and the baseband beamforming. In the absence of a limited feedback strategy, the estimated values of an accurate downlink channel the receiver's coefficient feedback could cause significant overhead and processing latency. For factory automation, the required end-to-end latency is expected to be less than 1 ms such that tolerable latency for deploying extended sweeping time of analog beam selection and channel coefficient feedback-based closed-loop hybrid beamforming/beam-tracking might be difficult. Consequently, limited feedback beamforming using a spatial diversity technique in conjunction with beam selection and a simplified digital domain codebook index [17] could be a desirable general solution for meeting the latency requirements in the physical layer.

In this paper, we propose a URLLC system using limited feedback frequency divided group beamforming with sparse space-frequency transmit diversity coded orthogonal frequency division multiplexing (OFDM). Motivated by Kaiser [18], parts of channel coding codeword are combined with space-frequency block code (SFBC) accommodating more than two antenna ports, allowing spatial transmit diversity (instead of duplicated eigenmode transmission of symbols in the multispatial stream) combined with beamforming via massive antenna elements. Through simulations, we show that the proposed structure of partially connected beamforming antenna groups to the number of frequency-separated RF chains (ports) enables diversity combining in frequency as well as a spatial domain with beamforming array gain. We emphasize that for a latency-effective URLLC physical layer design above 6 GHz systems, finding the balance between array gain and diversity order is the best course of action. We also demonstrate that adjusting the transmit power ratio of beamforming antenna groups through cooperative game theory with parameters obtained from the beam selection process and limited feedback further assists in acquiring signal-to-noise ratio (SNR) margin for improved link performance because beamforming antenna groups can be spatially separated.

The rest of the paper is organized as follows. In Section 2, we present the system model of the proposed frequency divided group beamforming transmits structure with low complexity transmit power control game, including preliminary results in Section 3; numerical performance results are presented for the proposed transmitter layout as well as a few reference systems. Finally, we draw concluding remarks in Section 4. The following notations are used throughout the essay. Let bold and upper case bold symbols represent vector and matrix, respectively, and $\mathbf{x}^*$ and $||\mathbf{x}||^2$ denote the conjugate transpose and the squared Euclidean norm of vector $\mathbf{x}$, respectively.

2 | SYSTEM DESCRIPTION

Reliability requirement beyond 5G NR URLLC at above 6 GHz is expected to be around BLER 10^{-9} at the 5th percentile SINR cumulative distribution function of the test environment [1], and it may require designing a physical layer acquiring both beamforming array gain and diversity to achieve minimal required SINR for reliability, since the target BLER is at an extremely low level. We describe a system to successfully acquire both diversity and array gain in a non-line-of-sight (NLoS) channel to satisfy the requirement of the beyond 5G NR URLLC scenario, where the maximum number of massive antenna elements at both bases and the mobile station are relatively limited.

2.1 | Received signal vector after baseband transform precoding and 2D analog vector steering

The following is a description of the baseband transmission process for the proposed sparse space-frequency

block code (SSFBC) system. As shown in Figure 1, a rate-matched channel, the codeword bit stream is modulated and then a complex symbol vector is formed. Symbol transform precoding block first duplicates input symbol $s(\cdot)$ and then applies permutation and conjugation as follows:

$$\begin{aligned} s'(k) &= z(k)\cdot[s_{\text{re}}(k+z(k)) - j\cdot s_{\text{im}}(k+z(k))] \\ z &= (-1)^k,\ k=0,\ 1,\ \ldots,\ C=Q-1 \end{aligned} \tag{1}$$

that two consecutive $N_s \times 1$ symbol vector $\mathbf{s} = [s(k), s'(k)]^{\text{T}}$ in frequency domain (i.e., $[\mathbf{s}_k, \mathbf{s}_{k+1}]$) form SFBC unit [19]. $s_{|\text{textre}}$ and s_{im} means real and imaginary part of symbol $s(\cdot)$, respectively. C refers to codeword length, and Q is the modulation order. The SFBC block is multiplexed with precoding matrix $\mathbf{F}_{\text{BB}}$ before conversion to OFDM waveform.

For simplicity, a subcarrier-wise multiple input multiple output (MIMO) channel is considered, which yields a received signal

$$\mathbf{y} = \mathbf{H}\mathbf{F}_{\text{RF}}\mathbf{F}_{\text{BB}}\mathbf{s} + \mathbf{n}, \tag{2}$$

where $\mathbf{y}$ is the $N_{\text{r}} \times 1$ receive vector, $\mathbf{H}$ is the $N_{\text{r}} \times N_{\text{t}}$ channel matrix, and $\mathbf{n}$ is the vector of additive Gaussian noise with i.i.distribution $\mathcal{CN}(0, N_0)$. $\mathbf{F}_{\text{BB}}$ is the transmitter baseband precoder composed of N_{s} by N_{s} spatial stream (ss) dimension. $\mathbf{F}_{\text{RF}}$ is the $N_{\text{t}} \times N_{\text{s}}$ transmitter RF precoder composed of 2D uniform planar arrays of steering vector $\mathbf{q}$ per N_{s} spatial stream dimension, expressed as

$$\mathbf{F}_{\text{RF}_{\theta,\phi}} = [\mathbf{q}\ \mathbf{q}]. \tag{3}$$

Given the calculated zenith angle of departure (ZoDs) and azimuth angle of departure (AoDs), each spatial stream deployed in cross-pole antenna placement is steered by vector $\mathbf{q}$ expressed as follows:

$$\begin{aligned} \mathbf{q} &= \mathbf{g}_{\phi_{\text{H}}} \otimes \mathbf{u}_{\theta_{\text{V}}},\ N_{\text{t}} = KL \\ \mathbf{u}_{\theta_{|\text{V},k}} &= \frac{1}{\sqrt{K}}\left[1,\ e^{j\pi 1\cos(\theta_{\text{V}})},\ \ldots,\ e^{j\pi(K-1)\cos(\theta_{\text{V}})}\right]^{\text{T}} \\ \mathbf{g}_{\phi_{\text{H}},l} &= \frac{1}{\sqrt{L}}\left[1,\ e^{j\pi 1\sin(\phi_{\text{H}})},\ \ldots,\ e^{j\pi(L-1)\sin(\phi_{\text{H}})}\right]^{\text{T}}, \end{aligned} \tag{4}$$

where $\otimes$ means Kronecker multiplication and K and L are the total number of antenna elements in the vertical and horizontal dimensions, respectively. $\mathbf{u}_{\theta_{\text{V}}}$ refers to discrete Fourier transform (DFT) weight vector in vertical direction, whereas $\mathbf{g}_{\phi_{\text{H}}}$ refers to phase shift weight direction in the horizontal direction. Interantenna spacing (either vertical or horizontal direction) of $\lambda/2$ is assumed. θ_{V} and ϕ_{H} are the estimated ZoD and AoD beam direction angle values, respectively. In the proposed system model, we set the vector size of $\mathbf{q}$ as N_{t}. Since cross-pole antennas are used to implement spatial stream separation, as shown in Figure 1, the array weight vector $\mathbf{q}$ for each N_{s} spatial stream is essentially the same.

The methods for finding the vector phase shift coefficients on analog beamforming/precoder follow the 5G NR beam sweeping concept. According to the NR specification, the base station may send the same

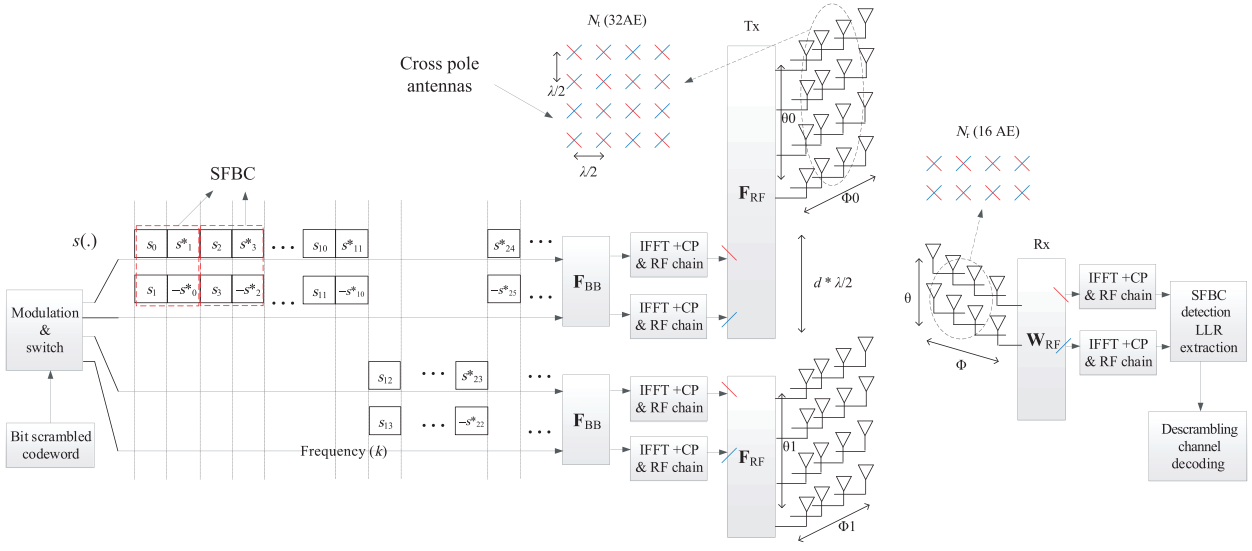

FIGURE 1 Transmitter structure of the proposed system with two beamforming/frequency-separated groups (panels) example; 64 with (32 for beamforming groups) and 16 antenna for transmitter and receiver elements (AE) are shown, respectively

synchronization signal block (SSB) up to 64 times in succession. The base station $\mathbf{F}_{\mathrm{RF}}$ sets a variety of preconfigured sets of two-dimensional phase shift values through this identical SSB transmission in the baseband, and the mobile station responds to the SSB time slot or instant that measured the highest receive power of the RS contained in the SSB slot structure. As such, the phase values θ_{V} and ϕ_{H} for each transmits beamforming group are determined.

$\mathbf{F}_{\mathrm{BB}}$ is composed of a simple precoding matrix and a connector that switches the input signal vector $\mathbf{s}(k)$ to different RF chains according to the frequency location. Depending on the $M(m=0,1,...,M-1)$ partially connected beamforming groups, the switching function for RF chain SFBC group domain can be expressed as $m=(k/f_{\mathrm{sub}})\bmod(N_{\mathrm{RF}}/2)$, where f_{sub} refers to frequency domain subband length. The baseband spatial layer is not increased by an increase in the RF chain or beamforming groups; it should be noted.

Simple transmit diversity using a cross-pole antenna configuration to maximize spatial channel gains make up the baseband structure. Two spatial streams are separated by a cross-pole configuration, as shown in Figure 1. While the instantaneous power due to random phases and transmit/receive ray coupling corresponding to azimuth and zenith may vary, the long-term channel power originating from each cross-pole is almost the same. Applying a precoder made of unit vectors is now possible, which may help to close the information gap between the mobile station's feedback and the eigenvalues of each spatial stream. In the most straight forward conventional close-loop beamforming method, the receiver measures composite channel $\mathbf{H}_{\mathrm{eff}}=\mathbf{H}\mathbf{F}_{\mathrm{RF}}$, and $\mathbf{F}_{|\mathrm{textBB}}$ can be derived by applying singular value decomposition (SVD)

$$\mathbf{H}_{\mathrm{eff}}=\mathbf{U}\Sigma\mathbf{V}^{\mathrm{H}}, \tag{5}$$

where $\mathbf{U}$ and $\mathbf{V}$ are unitary matrices. The receiver selects one from the finite beamforming precoder matrices

$$\mathbf{F}_{\mathrm{BB}}=Q_n(\mathbf{V})=[\mathbf{f}_0\mathbf{f}_1], \tag{6}$$

where $\mathbf{f}_0=[a,be^{j\varphi}]^{\mathrm{T}}$ and $\mathbf{f}_1=[b,-ae^{j\varphi}]^{\mathrm{T}}$ are vectors which are composed of quantized/normalized magnitude values a,b and quantized angle $\varphi\in[0,2\pi)$. Q_n is a quantization operator. From several solutions found for unitary matrices $\mathbf{U}$ and $\mathbf{V}$, an arbitrary phase value is multiplied by the columns of orthonormal vectors $\mathbf{f}_0$ and $\mathbf{f}_1$ to make the first row of $\mathbf{V}$ as a real number. At the receiver, baseband filter $\mathbf{W}_{\mathrm{BB}}=\mathbf{U}^{\mathrm{H}}$ is assumed.

Despite the known optimal performance of feeding back the precoding matrix $\mathbf{V}$ to the transmitter, it involves large overheads even if a highly compressed quantization process of $Q_n(\mathbf{V})$ is applied, and such could potentially impair the uplink channel reliability. Since the reliability of the proposed system is achieved by maximizing diversity, a different but marginally less efficient method of enhancing link performance could be achieved by lowering spatial correlation between SFBC layers. The spatial correlation could be assessed by channel condition number (*CN*), and to reduce the feedback information and receiver complexity, $\mathbf{F}_{\mathrm{BB}}=[\mathbf{f}_0\mathbf{f}_1]$ can be redefined as follows:

$$\begin{aligned}\mathbf{f}_0&=\left(\sqrt{2}\right)^{-\gamma}[1,\gamma e^{j\varphi_0}]^{\mathrm{T}}\\ \mathbf{f}_1&=\left(\sqrt{2}\right)^{-\gamma}[\gamma e^{j\varphi_1},1]^{\mathrm{T}}\end{aligned} \tag{7}$$

for minimizing *CN*, further removing the need for $\mathbf{W}_{\mathrm{BB}}$ at the cost of link performance. Instead of feeding back the $\mathbf{V}$, the receiver analyzes the net result of the eigenvalues by applying

$$\mathbf{H}_{\mathrm{eff}}\mathbf{F}_{\mathrm{BB}}=\bar{\mathbf{U}}\Sigma_{F_{\mathrm{BB}}}\bar{\mathbf{V}}^{\mathrm{H}}. \tag{8}$$

Predefined library of precoding matrices composed of finite combination values of φ_0 and φ_1 are compared, and they are matched to minimize the $CN=\lambda_{\max}/\lambda_{\min}$, $\lambda_{\min}\neq 0$ from the diagonal matrix $\Sigma_{F_{\mathrm{BB}}}$. Let γ be a binary value such that if not a single precoding matrix $\mathbf{F}_{\mathrm{BB}}$ from the predefined library lowers the *CN*, then $\gamma=0$. Limited feedback quantized values of φ_0,φ_1 and binary bit γ are fed back to the transmitter. For instance, the total overhead for SVD feedback would be a total of 24 bits but would only be 9 bits for the proposed system if we assumed approximately 10 bit per amplitude value and 4 bit for angular values. This translates to 62.5% feedback reduction in terms of lowering feedback report overhead in the uplink.

2.2 | Partially connected analog beamforming structure with unified array response vectors

It is well-known that there are two main categories for the architecture of RF chain-to-antenna mapping in hybrid beamforming: fully connected and partially connected. We suggest implementing a partially connected scheme rather than a fully connected antenna to RF chain architecture. As seen in Figure 1, having fewer analog parts and antennas per RF chain reduces array gain but increases transmit power thanks to partially connected structures for each antenna element and simpler hardware. The example architecture shown in Figure 1

intends two frequency regions and physical distance separation (i.e., $d\frac{\lambda}{2}$) per beamforming group (i.e., panels in Figure 2) to gather channel difference. The goal of this sparse space-frequency baseband structure and analog beamforming structure with partial connections is to increase diversity in the frequency and spatial domains. When it is extended to a multipoint transmission system (example in Figure 2), the probability of obtaining both lines of sight channel and ZoD/AoD angles closer to bore-sight increases.

The subbands in the even frequency regions of the example in Figure 1 are linked to the first RF chain and antenna group, while the other subbands in the odd frequency regions are linked to the second RF chain and antenna group. This makes it possible for each frequency-separated beamforming group to independently sweep the beam, and spatial diversification is caused by effective channel coefficients as a result of frequency-separated allocation. Because of the strict frequency region dependence of the proposed sparse frequency to spatial layer structure, diversity is provided at the expense of a lower transmit array gain. When compared with the fully connected frequency to the spatially dense case, which is later discussed in the numerical section, this frequency-separated and partially connected approach is shown to be more effective in terms of achieving higher diversity order in NLoS channels for URLLC applications while requiring lower SINR targeting BLER at 10^{-9}.

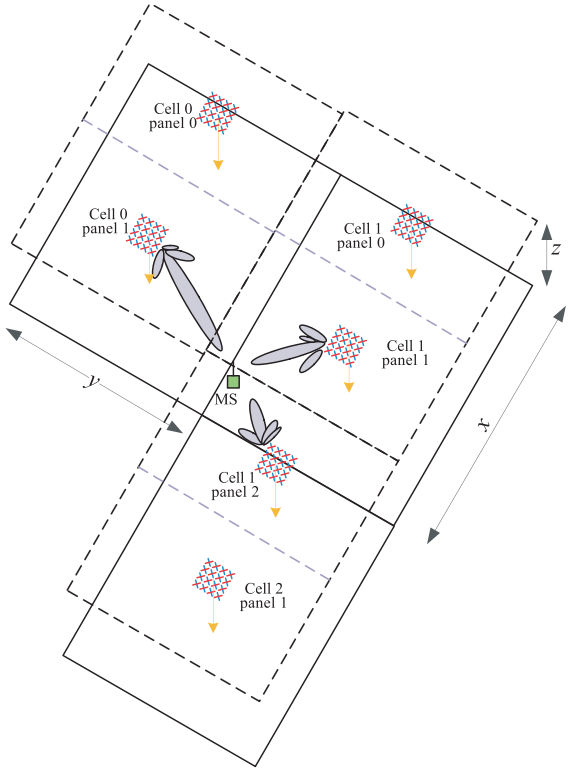

FIGURE 2 Multipoint transmission scheme for MS located at cell edge

Note that in Figure 1, beamforming groups are at least 2λ (assuming $d \geq 4$) apart. Because the beamforming groups are frequency-separated, the receive beamforming process for each baseband frequency region can be carried out independently, resulting in channel diversity. We assume that DFT-based steering angles in (4) for transmit and receive antennas are obtained from the beam selection process that AoD and ZoD can be implicitly showed to the transmitter in response to the strongest AoD/ZoD beam angle through periodically sending synchronization reference signal burst (SSB) during initial access and beam management phase, as well implemented in 5G NR [20, 21]. Such a beam selection procedure can be seen as a limited feedback beamforming method in and of itself.

2.3 | Power allocation method for distributed panel based intercell joint multipoint transmission

The transmitter structure of the suggested system is strictly single-user based, and the beam selection method focuses on delivering the greatest array gain. This could lead to interference between various users. Appropriate multiplexing and base station scheduling can allocate downlink/uplink resources while controlling intracell user interference. There are restrictions on how this DFT-based RF beamformer can handle interference from neighboring cells, and it can also significantly increase intercell interference for users who are situated at cell edges. As shown in Figure 2, cell edge users suffering from intercell interference by neighboring base stations can benefit from making the other base stations participate in the joint cooperative transmission. In 3GPP LTE, coordinated multipoint transmission and reception are used for this intercell multipoint transmission. The frequency divided group beamforming concept used in the proposed system enables each beamforming group to be logically and physically located in neighboring cells. Thus, when frequency bin regions are divided into three independent (but sharing a common codeword) beamforming groups, the transmitter structure of Figure 1 can be extended to Figure 2. In this way, cooperative transmission could be used to manage interference from nearby cells.

Participating base stations typically assume that channel state information (CSI) or channel quality indicator (CQI) is provided when allocating transmit power. Network sum capacity can be optimized by allocating the

proper power to each transmission reception point (TRP) (or distributed base station's panels) by reducing the user interference of noncooperating base stations or cooperating nonparticipating panels when CSI for all participating TRPs is provided. The multipoint transmission scheme can be viewed as distributed antenna system (DAS), and power allocation plays an important role in improving the channel capacity of DAS [22]. It has been extensively studied how to allocate power for a DAS system, and the majority of the suggested plans presuppose that transmitters are aware of the downlink CSI.

Conventional power allocation methods assume that exact CSI is available at the transmitter, but we propose replacing the exact full CSI feedback with transmit beam direction (i.e., ZoD/AoD) and CQI, which reduces feedback traffic significantly. A cooperative game is used to develop the solution for estimating the transmit power of participating TRPs, and the reduced feedback overhead for power control is used to determine the proper transmit power control for participating TRPs. With transmitter beam angle and CQI-based power allocation (ACPA), I base stations near the mobile station form a cooperating multipoint transmission set, and each base station's panel has a set of $P=\{P_i|P_0, P_1, ..., P_{I-1}\}$ bounded by $P_i \in [P_{\min}, P_{\max}]$. Then the utility function of the i-th TRP can be defined as follows:

$$\begin{aligned} &u_i(P_i,P_{\setminus i}) = \\ &\log_2\left(1+\frac{P_i\Omega_i(1-\beta)+\beta q_i+\sum_{\setminus i\in I}(P_{\setminus i}\Omega_{\setminus i}(1-\beta)+\beta q_{\setminus i})}{N_0}\right) \\ &-\log_2\left(1+\frac{\sum_{i\in I}P_{\setminus i}\Omega_{\setminus i}(1-\beta)+\beta q_{\setminus i}}{N_0}\right)-\alpha P_i \\ &=\log_2\left(1+\frac{P_i\Omega_i(1-\beta)+\beta q_i}{\sum_{\setminus i\in I}(P_{\setminus i}\Omega_{\setminus i}(1-\beta)+\beta q_{\setminus i})+N_0}\right)-\alpha P_i, \end{aligned} \tag{9}$$

where $P_{\setminus i}$ refers to the power of other base station's TRPs (panels) except i in the cooperating transmission set. N_0 is the noise power factor. α refers to the penalty of interference caused by the i-th TRP to other downlink channels, while the first term of (9) is the utility margin related to P_i. β is a weighting ratio of angle-based channel power and CQI level for determining the estimated channel gain of each TRPs. Ω_i is an estimated long-term channel gain factor originating from ZoD/AoD, expressed as [23]

$$\Omega_i = 10^{-\min\left[\min\left[12\left(\frac{ZoD_i-90^o}{65^o}\right),\ 30\right]+\min\left[12\left(\frac{AoD_i}{65^o}\right),\ 30\right],\ 30\right]/10}+\beta.$$

In nonideal intercell back haul case, current instantaneous $P_{\setminus i}$ are unknown to base station i, since the participating base station's $P_{\setminus i}$ of a panel is hard to track instantly due to numerous downlink beamformed scheduling situations. The initial power value for the cooperating TRPs' power is set to $P_{\max}/I$ due to the power allocation issue caused by the cooperating base station's panel's unknown transmit power information. Thus, (9) is modified to

$$\begin{aligned} u_i(P_i, P_{\setminus i}) = &\log_2\left(1+\frac{P_i\Omega_i(1-\beta)+\beta q_i}{\sum_{\setminus i\in I}\left(\frac{P_{\max}}{I}\Omega_{\setminus i}(1-\beta)+\beta q_{\setminus i}\right)+N_0}\right) \\ &-\alpha P_i, \end{aligned} \tag{10}$$

such that ZoD/AoD and CQI levels from other TRPs are gathered to the mobile station and then reported to the serving base station. q_i is the CQI level of the i-th mobile station's feedback. Then, each base station i's adjustment of its transmit power P_i to maximize the utility function yields

$$\begin{aligned} P_i^{\text{opt}} &= \text{argmax}\ u_i(P_i,P_{\setminus i}), P_i\in[P_{\min}, P_{\max}] \\ \text{s.t.}\quad &\alpha_{i,\min}<\alpha<\alpha_{i,\max}, P_{\max}\approx\sum_i^I P_i. \end{aligned} \tag{11}$$

We obtain P_i^{opt} by letting $[\partial u_i(P_i,P_{\setminus i})]/\partial P_i=0$ and searching α that satisfies the constrains of (11), then we have

$$P_i=\frac{1}{\alpha\ \ln\ 2}-\frac{\sum_{\setminus i\in I}\left(\frac{P_{\max}}{I}\Omega_{\setminus i}(1-\beta)+\beta q_{\setminus i}\right)+N_0}{\Omega_i(1-\beta)+\beta q_i}. \tag{12}$$

If $P_i^{\text{opt}}<=0$, then $P_i^{\text{opt}}=0$. The actual transmit power P_i is affected by the upper and lower bounds; therefore, α is bounded by

$$\begin{aligned} \alpha_{i,\min} &:= \frac{1}{\ln\ 2}\ \ P_{\max}+\frac{\sum_{\setminus i\in I}\left(\frac{P_{\max}}{I}\Omega_{\setminus i}(1-\beta)+\beta q_{\setminus i}\right)+N_0}{\Omega_i(1-\beta)+\beta q_i}\Bigg)^{-1} \\ \alpha_{i,\max} &:= \frac{1}{\ln\ 2}\ \ P_{\min}+\frac{\sum_{\setminus i\in I}\left(\frac{P_{\max}}{I}\Omega_{\setminus i}(1-\beta)+\beta q_{\setminus i}\right)+N_0}{\Omega_i(1-\beta)+\beta q_i}\Bigg)^{-1}. \end{aligned} \tag{13}$$

As an example similar to Figure 2, when ZoD/AoD of three participating TRPs have $ZoD_0/AoD_0=130^\circ/60^\circ$, $ZoD_1/AoD_1=100^\circ/10^\circ$, $ZoD_2/AoD_2=110^\circ/20^\circ$ and $N_0=0.02$, with all the same CQI value q_i of 0.5, $\beta=0.5, \alpha=0.895$, then we obtain $P_0=0.06, P_1=0.61$, $P_2=0.33$. Both β and q_i are normalized values. $P_{\max}=10^\circ$ and $P_{\min}=10^{-3}$ are assumed. And the constraint in (11) is met. When CQI is not available, the

proposed power allocation scheme can still be functional by setting $\beta = 0$. Be aware that the suggested method can be used in the single cell multipanel transmission case. This would make $P_{\setminus i}$ instantly known to base station i.

2.4 | Receiver processing

At the receiver, receive beamforming steering vector $\mathbf{W}_{\mathrm{RF}}$ of N_{r} x N_{RF} similar to (4) combines all the signals from N_{t} antenna elements that are convoluted with channel and then mapped to RF chain input signal. The receiver measures the received power of the RS for the receiver side analog beam sweeping operation during the transmit beamforming sweeping time. Assuming that the transmitter side beamforming weight during a specific sweeping interval is fixed, the receive analog beamformer applies preconfigured set of phase shift vector for $\theta_{\mathrm{V,ZoA}}$ and $\phi_{\mathrm{H,\,AoA}}$. Due to the proposed frequency-separated beamforming system structure, the receiver can perform simultaneous $\theta_{\mathrm{V,ZoA}}$ and $\phi_{\mathrm{H,\,AoA}}$ estimation per transmitter beamforming groups. The array response vector calculates the ZoA/AoA following baseband fast Fourier transform (FFT) operation and baseband precoder counterpart filtering. Then, we obtain a signal in the frequency domain

$$\begin{aligned}\mathbf{r}_k &= \mathbf{W}_{\mathrm{BB}}\mathbf{W}_{\mathrm{RF}}\mathbf{y}_k \\ &= \mathbf{W}_{\mathrm{BB}}\mathbf{W}_{\mathrm{RF}}\mathbf{H}\mathbf{F}_{\mathrm{RF}}\mathbf{F}_{\mathrm{BB}}\mathbf{s} + \mathbf{W}_{\mathrm{BB}}\mathbf{W}_{\mathrm{RF}}\mathbf{n},\end{aligned} \tag{14}$$

where $\mathbf{W}_{\mathrm{BB}} = \mathbf{U}^{\mathrm{H}}$ if quantized version of unitary matrix $\mathbf{V}$ is set for $\mathbf{F}_{\mathrm{BB}}$; otherwise, $\mathbf{W}_{\mathrm{BB}}$ can be set as identity matrix $\mathbf{I}$, as proposed by minimizing CN of limited feedback version.

The issue of estimating the SFBC coded transmit signal from receive vectors from two subcarriers is one that the receiver attempts to resolve by searching

$$\arg \min_{\hat{\mathbf{s}}=[s_0,s_1]^{\mathrm{T}} \in Q} ||\mathbf{r}_{2k} + \mathbf{r}^*_{2k+1} - \mathbf{H}_{\mathrm{eff},2k}\hat{\mathbf{s}} - \mathbf{H}^*_{\mathrm{eff},2k+1}\hat{\mathbf{s}}^*||^2. \tag{15}$$

Here, transposed transmission of SFBC block unit in (1) $\mathbf{S}_{\mathrm{SFBC}} = [\mathbf{s}_k, \mathbf{s}_{k+1}]^{\mathrm{T}}$ is assumed. There are other linear detection methods available for estimating SFBC coded symbols. The interference may, however, result in a BLER floor because of the presence of channel frequency response (CFR) selectivity even between neighboring subcarriers. Without a method for handling the interference brought on by subcarrier CFR difference, such zero-forcing and/or minimum mean square estimation-type receivers might not be appropriate for URLLC systems.

3 | NUMERICAL RESULTS

The results of link-level simulation using the cluster delay line (CDL) channel model and various transmit antenna placement configurations are compared in this section. The evaluation assumptions and parameters are given as follows: center frequency of 30 GHz is applied, 240 kHz subcarrier spacing, mini-slot of two OFDM symbols (0.01042 ms of transmission time interval [TTI]), 491.52 MHz system bandwidth, 100 RBs (1200 subcarriers out of FFT size 2048) assigned, and 32 bytes of payload size is assumed. The front-loaded demodulation reference signal (DMRS) of one OFDM symbol is occupied despite the assumption of perfect channel estimation, so the other OFDM symbol is used for payload transmission. NR low-density parity check (LDPC) base graph 2 [24] is applied for channel coding. CDL-A channel model [23] with an average delay spread of 29 ns is configured. In default, ZoD ($90^\circ \le \theta \le 135^\circ$, AoD ($-60^\circ \le \theta \le 60^\circ$, ZoA ($45^\circ \le \theta \le 90^\circ$), and AoA ($-180^\circ \le \theta \le 180^\circ$) angle spreads are considered, as described in an earlier study [25]. The base station vertical tilting degree of 20° is assumed. By aligning with the angles of the strongest cluster in the CDL-A channel model, the beamforming technique is used at both the transmitter and the receiver (i.e., the second cluster).

Some of the simulation configurations are set experimentally to observe the best reference performance for comparisons. In these circumstances, it is assumed that the transmit ZoD, AoD, ZoA, and AoA are configured with the receiver at bore-sight and that angular spread is not used. The transmitter is equipped with 4 × 8 × 2 (V × H × Pol.) antenna configuration. An example of two beamforming groups correlated with frequency division is shown in Figure 1. Both vertical and horizontal dimensions are used when virtualizing antenna array ports. As shown in Figure 1, $2 \times 4 \times 2$ (V × H × Pol.) receive antenna configuration is applied. As an experimental case, the impact of angular spreads without receive beamforming is observed and contrasted with that of receive beamforming with bore-sight ZoA/AoA using a $1 \times 1 \times 2$ (V × H × Pol.) antenna configuration.

We first compare the effectiveness of obtaining diversity order only with SSFBC structure under ZoD/AoD/ZoA/AoA bore-sight angle in NLoS channel conditions. As a result, angular spread and beamforming are not applied in Figure 4. To compare the efficiency in obtaining the diversity order, the number of transmit RF chains is set to either 8 or 16. When eight RF chains are assumed, eight AEs are tied with one RF chain, whereas four AEs are assigned for 16 RF chain cases. Default antenna spacing of $\lambda/2$ among antenna elements is assumed.

The reference scheme, shown in Figure 3, has each antenna port of increasing time delayed (or cyclic delayed diversity) transmit diversity [26] structure with known bit/symbol level scrambled the sequence in the spatial domain. This scrambling of the spatial levels can also be seen as the spreading of the spatial levels (noted as CDD spreaded). There is a direct correlation between the number of transmit RF chains and the diversity order of the reference and proposed SSFBC schemes. It is observed in Figure 4 that physical antenna spacing among horizontal elements in the CDL-A channel model, corresponding to number of transmitting RF chains, leads to higher achievable diversity order. To distinguish the distance between antenna port (RF chain) units, the horizontal spacing is varied, while the vertical spacing is maintained at $\lambda/2$.This suggests that channel diversity and increased antenna spacing between various antenna ports are related. As a performance reference, we plot normal approximation [27] for theoretical lower bound of having two receive antenna ports. We observe that in terms of the total number of antenna elements/ports configuration and antenna element spacing, the proposed scheme's trend is similar to that of the baseline reference scheme. However, the proposed scheme exploits not only the diversity from massive transmit ports but also the transmitter side maximal ratio combining gain integrated into the receive ML soft metric in (15). In comparison with the baseline reference scheme, the proposed SSFBC system achieves an SNR gain of approximately 1.3 dB given the same number of transmit and receive antennas.

A few experimental cases are covered to observe how angular spread and beamforming affect the diversity order with $N_{RF} = 16$. All receiver antennas in Figure 5 are restricted to two AEs. Therefore, receiving BF cannot be used. We presume that there is no delay between the feedback information from the receiver and the channel variation. Precoding matrix $\mathbf{F}_{BB}$ with reduced overhead version targeting lower *CN* is applied. This has been set up specifically to examine the impact of beamforming and angular spread on the performance of BLER at the transmitter side. The diversity order in the experimental cases depicted in Figure 5 for the fixed ZoD/AoD/ZoA (AoA with angular spread) case is almost identical to the case with no beamforming and an ideal fixed bore-sight but no angular spread. As shown in Figure 5, angular spread causes SNR loss due to the antenna field pattern model in a previous research [23]. Even with the use of ZoD/AoD beamforming, further SNR loss is seen when

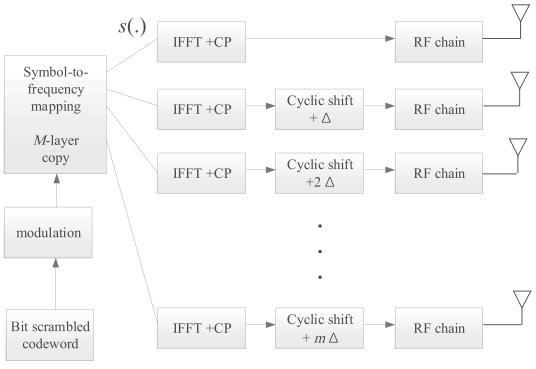

FIGURE 3 Cyclic delay diversity (CDD) transmission as a baseline multi-radio frequency (RF) chain reference scheme

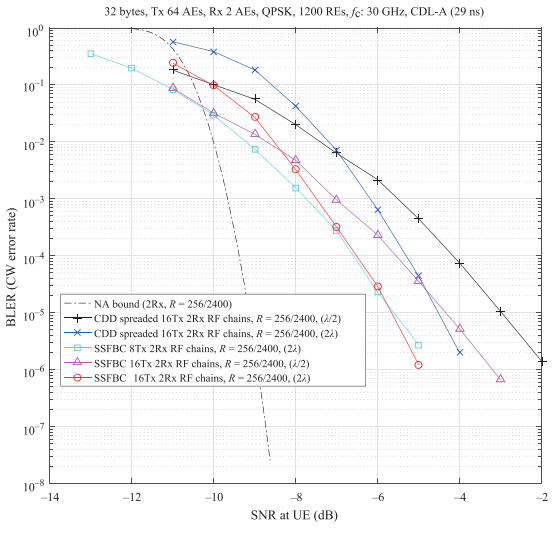

FIGURE 4 Comparison of transmit diversity schemes with fixed bore-sight angle $N_t = 64$ and $N_r = 2$ in cluster delay line (CDL)-A channel model. All schemes use quadrature phase shift keying (QPSK) for symbol modulation

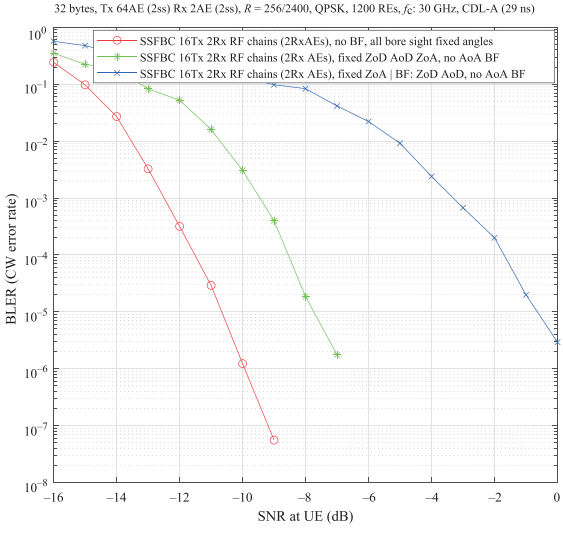

FIGURE 5 Comparison of experimental beamforming and angular spread setting with $N_t = 64$ and $N_r = 2$ in CDL-A channel model. All schemes use quadrature phase shift keying (QPSK) for symbol modulation

the additional angular spread is applied to ZoD/AoD. The diversity order appears to be close to the ideal case, but the results show that using numerous RF chains to increase diversity order causes a sizable array gain loss.

Even with ZoD/AoD beamforming, additional angular spread causes SNR loss. Although the diversity order appears to be close to the ideal case, the results show that increasing the diversity order by utilizing many RF chains results in a significant array gain loss. There are four cases (i.e., $N_{RF} = 2$, 4, 8, and 16) that RF chain-to-AE beamforming groups are considered such that $N_{AE} = 32/N_{RF}$ per beamforming group is maintained. Independent phase values for θ_V and φ_H per beamforming group (corresponds to baseband frequency regions) are assumed, according to N_{RF} values. The distance between beamforming groups is set to at least $d \geq 4$ apart. When the beam selection method for beamforming is used, all beamforming groups are set to have the same identical **q** weights, implying a simplified beamforming procedural step. Despite this, due to frequency subband separation, the proposed system can still perform independent/simultaneous beamforming per group at the transmitter side. We first plot the simulation result of SVD (Equation 6) based on two transmitters and two receivers N_{RF} ports configuration, as a reference scheme. Before baseband precoding, both the transmitter and receiver sides use the analog beamforming procedure described in Sections 2.1 and 2.4. In terms of both array gain and diversity order, the reference SVD-based hybrid beamforming scheme provides the best overall performance. In Figure 6, another baseline SFBC scheme is configured with two RF chains for both transmitter and receiver,

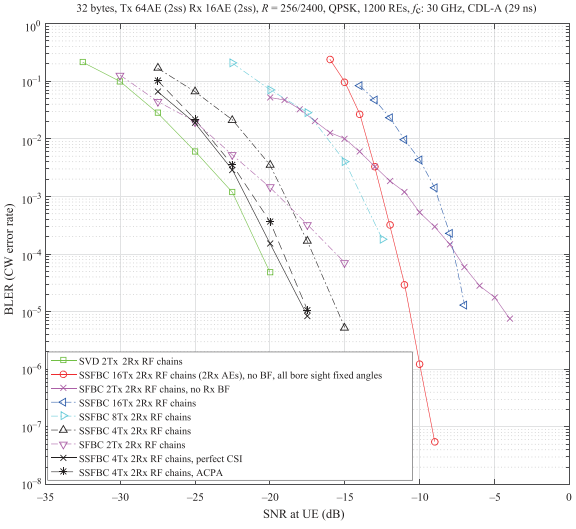

FIGURE 6 Comparison of radio frequency (RF) chain/frequency grouping with angular spreads $N_t = 64$ and $N_r = 16$ in cluster delay line (CDL)-A channel model. All schemes use quadrature phase shift keying (QPSK) for symbol modulation

and it shows a larger array gain, compared with the proposed method. In contrast to the example in Figure 1, the baseline reference SFBC scheme has no frequency divided beamforming groups, and all antenna elements are fully connected to each N_{RF} RF chain. When two beamforming groups are formed with $N_{AE} = 16$ (physically 16 AEs but logically 32 AEs) per RF chain, as shown in Figure 1, array gain loss is present, but an increase in diversity order is observed in the proposed SSFBC system. For $N_{RF} = 8$ and 16, a general trend of trade-off relation between array gain and diversity order is observed. In the URLLC scenario, it is obvious that a good balance between array gain and diversity order for the SSFBC system must be found, and in the CDL-A NLoS case, the proposed limited feedback-based SSFBC transmission scheme with four RF chains appears to be sufficient to achieve both array gain and higher diversity order. Furthermore, it exhibits a diversity order that is similar to the reference SVD scheme with a slight SNR shift difference. Similar to the example in Figure 2, we used multipoint transmission with an ACPA scheme to two TRPs that are close to the mobile station (i.e., Cell 0 and Cell 1). In this case, the y-axis angular spread is given, while the x-axis is fixed, and the number of transmitter and receiver RF chains is 4 and 2, respectively, because two beamforming/frequency-allocation groups are assumed. In the multipoint transmission scenario, it is assumed that accurate ZoD/AoD (no CQI: $\beta = 0$) of the counterpart cooperating base station is exchanged via mobile station. Further analysis of proposed power allocation in link performance reveals that not only is diversity order maintained (when compared with a single base station case) but additional SNR gain is also achieved due to appropriate transmit power management based on ZoD/AoD. As shown in Figure 6, it is compared with the known perfect downlink CSI case. Long-term ZoD/AoD information is found to be a suitable alternative information for estimating downlink CSI in spatially sparse scattered channels, as the link performance gap between perfect CSI and the proposed solution appears to be narrow. Obtaining downlink CSI from serving and cooperating base station TRPs is estimated to have a high overhead, whereas gathering ZoD/AoD (with/without CQI) angle information from TRPs is a more cost effective power allocation solution.

4 | CONCLUSION

In this paper, we proposed a URLLC system with high reliability and low overhead that is based on limited feedback frequency divided partially connected hybrid group beamforming with sparse space-frequency transmit

diversity coded OFDM. The proposed sparse frequency to spatial layer structure makes the beamforming antenna group strictly frequency region dependent and provides diversity for URLLC systems requiring very low BLER level, at the cost of reduced transmit array gain. Link-level simulations show that the proposed scheme achieves diversity order and array gain by grouping a sufficient number of frequency-separated beamforming units and thus provides reliability in a spatially sparse NLoS channel. When no downlink CSI is available for TRPs' power adjustment, the proposed low complexity frequency-separated beamforming with ACPA performs reasonably well in an intercell multipoint transmission scenario. The combination of frequency-separated beamforming groups with a limited feedback structure of beam selection and baseband precoding may offer a delay efficient and low complexity solution for above 6 GHz URLLC systems using hybrid beamforming.

ACKNOWLEDGMENTS

This work was supported by the Institute of Information and communications Technology Planning and Evaluation (IITP) grant funded by the Korea government (MSIT) (no. 2018-0-00218, Speciality Laboratory for Wireless Backhaul Communications based on Very High Frequency).

CONFLICT OF INTEREST

The authors declare that there are no conflicts of interest.

ORCID

Chanho Yoon https://orcid.org/0000-0001-6421-820X
Woncheol Cho https://orcid.org/0000-0001-7787-1101

REFERENCES

1. Report ITU-R M.2412-0, *Guidelines for evaluation of radio interface technologies for IMT-2020*. Tech. report. ITU-R, 2017.
2. METIS, *Mobile and wireless communications Enablers for Twenty-twenty (2020) Information Society, Deliverable d1.1 scenarios, requirements and KPIs for 5G mobile and wireless systems*, Tech. report, 2013.
3. M. Bennis, M. Debbah, and H. V. Poor, *Ultrareliable and low-latency wireless communication: Tail, risk, and scale*, Proc. IEEE **106** (2018), no. 10, 1834–1853.
4. G. Berardinelli, N. H. Mahmood, I. Rodriguez, and P. Mogensen, *Beyond 5G wireless IRT for industry 4.0: Design principles and spectrum aspects*, (Proc. of IEEE Globecom Workshops, Abu Dhabi, United Arab Emirates), 2018, pp. 1–6.
5. N. Brahmi, O. N. C. Yilmaz, K. Wang, Helmersson, S. A. Asharf, and J. Torsner, *Deployment strategies for ultra-reliable and low-latency communication in factory automation*, (Proc. of IEEE Globecom Workshops, San Diego, USA), 2015, pp. 1–6.
6. B. Holfed, D. Wieruch, T. Wirth, L. Thiele, S. A. Ashraf, J. Huschke, I. Aktas, and J. Ansari, *Wirelss communication for factory automation: An opportunity for LTE and 5G systems*, IEEE Commun. Mag. **54** (2016), no. 6, 361–343.
7. J. Sachs, G. Wikstrom, T. Dudda, R. Baldemair, and K. Kittichokechai, *5G radio network design for ultra-reliable low-latency communication*, IEEE Netw. **32** (2018), no. 2, 24–31.
8. J. Sachs, L. A. A. Andersson, J. Araújo, C. Curescu, J. Lundsjö, G. Rune, E. Steinbach, and G. Wikström, *Adaptive 5G low-latency communication for tactile internet services*, Proc. of IEEE **107** (2019), no. 2, 325–349.
9. O. E. Ayach, S. Rajagopal, S. Abu-Surra, Z. Pi, and R. W. Heath, *Spatially sparse precoding in millimeter wave MIMO systems*, IEEE Trans. Wireless Commun. **13** (2014), no. 3, 1499–1513.
10. H. Imori, G. T. F. D. Abreu, O. Taghizadeh, R-A. Stoica, T. Hara, and K. Ishibashi, *A stochastic gradient descent approach for hybrid mmWave beamforming with blockage and CSI-error robustness*, IEEE Acesss **9** (2021), 74471–74487.
11. R. Mendez-Rial, C. Rusu, N. Gonzalez-Prelcic, A. Alkhateeb, and R. W. Heath, *Hybrid MIMO architectures for millimeter wave communications: Phase shifters or switches?* IEEE Access **4** (2016), 247–267.
12. P. Ni, R. Liu, M. Li, and Q. Liu, *User association and hybrid beamforming designs for cooperative mmWave MIMO systems*, IEEE Trans. Sig. Info. Process over Networks **8** (2022), 641–654.
13. L. Pang, W. Wu, Y. Zhang, Y. Yuan, Y. Chen, A. Wang, and J. Li, *Joint power allocation and hybrid beamforming for downlink mmWave-NOMA systems*, IEEE Trans. Vehicular Tech. **70** (2021), no. 10, 10173–10184.
14. S. Park, A. Alkhateeb, and R. W. Heath, *Dynamic subarrays for hybrid precoding in wideband mmwave MIMO systems*, IEEE Trans. Wireless Commnun. **16** (2017), no. 5, 2907–2920.
15. F. Sohrabi and W. Yu, *Hybrid digital and analog beamforming design for large-scale antenna arrays*, IEEE J. Sel. Topics Signal Process. **10** (2016), no. 3, 501–513.
16. X. Yu, J.-C. Shen, J. Zhang, and K. B. Letaief, *Alternating minimization algorithms for hybrid precoding in millimeter wave MIMO systems*, IEEE J. Sel. Topics Signal Process. **10** (2016), no. 3, 485–500.
17. N. A. Johansson, Y.-P. E. Wang, E. Eriksson, and M. Hessler, *Radio access for ultra-reliable and low-latency 5G communications*, (IEEE International Conference on Communications (ICC) Workshop on 5G & Beyond - Enabling Technologies and Applications, London, UK), 2015, pp. 1184–1189.
18. S. Kaiser, *Spatial transmit diversity techniques for broadband OFDM systems*, (Proc. of IEEE Globecom, San Francisco, USA), 2000, pp. 1824–1828.
19. S. M. Alamouti, *A simple transmit diversity technique for wireless communications*, IEEE J. Sel. Areas Commun. **16** (1998), no. 8, 1451–1458.
20. J. Liu, K. Au, A. Maaref, J. Luo, H. Baligh, H. Tong, A. Chassaigne, and J. Lorca, *Initial access, mobility, and user-centric multi-beam operation in 5G New Radio*, IEEE Commun. Magazine **56** (2018), no. 3, 35–41.
21. 3GPP specification TS 38.213, 3GPP; TSG RAN; NR; physical layer procedures for control (release 17).
22. X. Chen, X. Xu, and X. Tao, *Energy efficient power allocation in generalized distributed antenna system*, IEEE Commnun. Lett. **16** (2017), no. 7, 1022–1025.

23. 3GPP (3rd generation partnerhsip project: https://www.3gpp.org/), *Study on channel model for frequencies from 0 to 100 GHz (Release 15)*, 3GPP; TR; 38.901. Tech. report, 2019. https://portal.3gpp.org/desktopmodules/Specifications/SpecificationDetails.aspx?specificationId=3173
24. 3GPP specification TS 38.212, *3GPP; TSG RAN; NR; multiplexing and channel coding*.
25. R1-1701823, *Evaluation assumptions for Phase 1 NR MIMO link level calibration*.
26. IEEE 802.11, *Part 11: Wireless LAN medium access control (MAC) and physical layer (PHY) specifications*.
27. Y. Polyanskiy, H. V. Poor, and S. Verdu, *Channel coding rate in the finite blocklength regime*, IEEE Trans. Inf. Theory **56** (2010), no. 5, 2307–2359.

AUTHOR BIOGRAPHIES

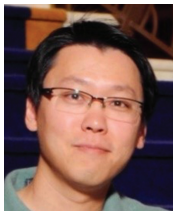

Chanho Yoon received the BS degree from Korea University, Seoul, Republic of Korea in 2003, and MS and PhD degrees both in Electrical Engineering from Korea Advanced Institute of Science and Technology, Daejeon, Republic of Korea, respectively, in 2005 and 2011. He has been with Electronics and Telecommunications Research Institute (ETRI) since 2005. From 2014 to 2019, he had participated in the 3GPP standardization of 5G NR as a delegate of ETRI. His research interests include 6G technologies with main focus in the physical layer aspects of radio access covering beamformed multi-antenna joint transmission combined with error-control coding techniques and their application in ultra-reliable communications and communication systems engineering.

Woncheol Cho received the BS and MS degrees in Information and Communications Engineering from Daegu Gyeongbuk Institute of Science and Technology, Daegu, Republic of Korea, in 2018 and 2020, respectively. He is currently a researcher with Electronics and Telecommunications Research Institute, Daejeon, Republic of Korea. His research interests include coded modulation and multi-point transmission.

Kapseok Chang received the PhD degree in Information and Communications Engineering from the Korea Advanced Institute of Science and Technology, Daejeon, Republic of Korea, in 2005, respectively. Since July 2005, he has been with Electronics and Telecommunications Research Institute (ETRI), Daejeon, Republic of Korea as a full-time senior researcher. Since September 2009, he has also been an associate professor of Mobile Communication and Digital Broadcasting Engineering with University of Science and Technology, Republic of Korea. From March 2011 to February 2013, he was with the School of Engineering Science, Simon Fraser University, Burnaby, Canada as a visiting professor. His research interests include smart antennas, OFDM, synchronization, interference cancellation, in-band full-duplex (IFD) realization, and cellular IoT system. He performed the standardization activities of 3GPP LTE (2005 - 2007) and IEEE 802.11ad (2009 - 2010), developing the prototype of IFD system (2014 - 2015). Dr. Chang was the recipient of the Brain Korea Scholarship, during his PhD. He was the recipient of the Certificate of Appreciation, the Day of the Inventions, and the Best Patent Award, from IEEE 802.11ad (2012), Korean Ministry of Commerce, Industry and Energy (2018), and ETRI (2019), respectively.

Young-Jo Ko received the BS, MS and PhD degrees in Physics from Korea Advanced Institute of Science and Technology, Daejeon, Republic of Korea, in 1992, 1994, and 1998, respectively. He joined Electronics and Telecommunications Research Institute (ETRI) in March, 1998. Since 2002, he has been working on mobile communications at ETRI. From 2005 to 2014, he participated in the development of early versions of LTE/LTE-Advanced systems and also participated in the 3GPP standardization of LTE/LTE-Advanced as a main delegate of ETRI. He is currently director of 6G Wireless Technology Research Section in Mobile Communication Research Division at ETRI, and serves as chairman of the Technology Committee of 5G Forum in Korea. His research interests, in recent years, include 5G New Radio and beyond, and 6G technologies, with his main focus lying in the physical layer aspects of radio access.

How to cite this article: C. Yoon, W. Cho, K. Chang, and Y.-J. Ko, *Frequency divided group beamforming with sparse space-frequency code for above 6 GHz URLLC systems*, ETRI Journal **44** (2022), 925–935. https://doi.org/10.4218/etrij.2022-0207